

See discussions, stats, and author profiles for this publication at: <https://www.researchgate.net/publication/323227343>

[18F]AV-1451 tau-PET and primary progressive aphasia

Article in *Annals of Neurology* · February 2018

DOI: 10.1002/ana.25183

CITATIONS

21

READS

63

19 authors, including:



Hugo Botha

Mayo Foundation for Medical Education and Research

75 PUBLICATIONS 565 CITATIONS

[SEE PROFILE](#)



Christopher G. Schwarz

Mayo Foundation for Medical Education and Research

169 PUBLICATIONS 1,993 CITATIONS

[SEE PROFILE](#)



Joseph R Duffy

Mayo Foundation for Medical Education and Research

226 PUBLICATIONS 6,427 CITATIONS

[SEE PROFILE](#)



Heather Clark

Mayo Foundation for Medical Education and Research

72 PUBLICATIONS 1,393 CITATIONS

[SEE PROFILE](#)

Some of the authors of this publication are also working on these related projects:




REM Sleep Behavior Disorder [View project](#)



New method for diagnosing acquired apraxia of speech - <http://goo.gl/J429Ca> [View project](#)

[¹⁸F]AV-1451 Tau-PET and Primary Progressive Aphasia

Keith A. Josephs, MD, MST, MSc,¹ Peter R. Martin, MS,³ Hugo Botha, MD,¹
Christopher G. Schwarz, PhD ,⁶ Joseph R. Duffy, PhD,² Heather M. Clark, PhD,²
Mary M. Machulda, PhD,⁴ Jonathan Graff-Radford, MD,¹
Stephen D. Weigand, MS,³ Matthew L. Senjem, MS,^{5,6} Rene L. Utianski, PhD,²
Daniel A. Drubach, MD,¹ Bradley F. Boeve, MD,¹ David T. Jones, MD, PhD,¹
David S. Knopman, MD,¹ Ronald C. Petersen, MD, PhD,¹ Clifford R. Jack Jr, MD,⁶
Val J. Lowe, MD,⁷ and Jennifer L. Whitwell, PhD⁶

Objectives: To assess [¹⁸F]AV-1451 tau-PET (positron emission tomography) uptake patterns across the primary progressive aphasia (PPA) variants (logopenic, semantic, and agrammatic), examine regional uptake patterns of [¹⁸F]AV-1451 independent of clinical diagnosis, and compare the diagnostic utility of [¹⁸F]AV-1451, [¹⁸F]-fluorodeoxyglucose (FDG)-PET and MRI (magnetic resonance imaging) to differentiate the PPA variants.

Methods: We performed statistical parametric mapping of [¹⁸F]AV-1451 across 40 PPA patients (logopenic-PPA = 14, semantic-PPA = 13, and agrammatic-PPA = 13) compared to 80 cognitively normal, Pittsburgh compound B–negative controls, age and gender matched 2:1. Principal component analysis of regional [¹⁸F]AV-1451 tau-PET standard uptake value ratio was performed to understand underlying patterns of [¹⁸F]AV-1451 uptake independent of clinical diagnosis. Penalized multinomial regression analyses were utilized to assess diagnostic utility.

Results: Logopenic-PPA showed striking uptake throughout neocortex, particularly temporoparietal, compared to controls, semantic-PPA, and agrammatic-PPA. Semantic-PPA and agrammatic-PPA showed milder patterns of focal [¹⁸F]AV-1451 uptake. Semantic-PPA showed elevated uptake (left>right) in anteromedial temporal lobes, compared to controls and agrammatic-PPA. Agrammatic-PPA showed elevated uptake (left>right) throughout prefrontal white matter and in subcortical gray matter structures, compared to controls and semantic-PPA. The principal component analysis of regional [¹⁸F]AV-1451 indicated two primary dimensions, a severity dimension that distinguished logopenic-PPA from agrammatic-PPA and semantic-PPA, and a frontal versus temporal contrast that distinguishes agrammatic-PPA and semantic-PPA cases. Diagnostic utility of [¹⁸F]AV-1451 was superior to MRI and at least equal to FDG-PET.

Interpretation: [¹⁸F]AV-1451 binding characteristics differ across the PPA variants and were excellent at distinguishing between the variants. [¹⁸F]AV-1451 binding characteristics were as good or better than other brain imaging modalities utilized in clinical practice, suggesting that [¹⁸F]AV-1451 may have clinical diagnostic utility in PPA.

ANN NEUROL 2018;00:000–000

Primary progressive aphasia (PPA) is an umbrella term that encompasses a group of neurodegenerative syndromes characterized by varying combinations of progressive language impairments.^{1,2} Three clinical variants of PPA have been well described and are well recognized³:

the agrammatic/nonfluent variant (agPPA) characterized by grammatical errors in speech and writing and sometimes associated with apraxia of speech⁴; the semantic variant (svPPA) characterized by grammatically and prosodically normal (ie, fluent) speech with poor naming

View this article online at wileyonlinelibrary.com. DOI: 10.1002/ana.25183

Received Nov 17, 2017, and in revised form Feb 12, 2018. Accepted for publication Feb 13, 2018.

Address correspondence to Prof Keith A. Josephs, Behavioral Neurology & Movement Disorders, Mayo Clinic, College of Medicine, 200 1st Street Southwest, Rochester, MN 55905. E-mail: josephs.keith@mayo.edu

From the Departments of ¹Behavioral Neurology and ²Speech Pathology (Neurology), ³Health Science Research (Biostatistics), ⁴Neuropsychology (Psychiatry), ⁵Information Technology, and ⁶Neuroradiology and ⁷Nuclear Medicine (Radiology), Mayo Clinic, Rochester, MN.

from loss of knowledge about the meaning of words; and the logopenic variant (lvPPA) characterized by hesitant speech from word retrieval problems, poor sentence repetition from impairment of working memory, and phonological errors.

Pathological studies have demonstrated that PPA is associated with a number of different abnormal cellular proteins that do not have perfect associations with the three PPA variants.^{4–8} One such protein is the microtubule-associated protein, tau, which is the most common abnormal protein found in the brains of patients with PPA.⁶ Tau is an important protein that has been linked to the neurodegenerative process in many diseases. Differential splicing of three exons in the tau gene yields three different isoforms of abnormally deposited tau in neurodegenerative diseases⁹: tau with predominantly four microtubule binding domains (4R tau); tau with three microtubule binding domains (3R tau); and tau with almost equal amounts of both (3R+4R tau). Understanding tau isoform deposition is important in PPA because pathological studies have shown an association between lvPPA and 3R+4R tau, and an association between agPPA and 4R tau.^{4–8} The svPPA variant is rarely associated with tau isoforms^{6,10} and is more commonly associated with another protein, the TAR DNA binding protein of 43 kDa (TDP-43).^{6,8,10}

With that said, pathological studies are limited by sampling small pieces of brain tissue and therefore cannot reveal patterns of tau deposition across the whole brain in PPA variants. Recently, tau PET (positron emission tomography) imaging has become available, which allows for assessment of tau deposition across the entire brain during life. One imaging ligand, [¹⁸F]AV-1451 (formerly 18F-T807), has been shown to specifically bind to tau in humans.¹¹ More recently, with autoradiographic studies, it has been shown that [¹⁸F]AV-1451 binds robustly to 3R+4R tau, whereas the binding to 4R tau is inconclusive.^{12–16} No neuroimaging studies have investigated tau-PET uptake across all three PPA variants. Hence, binding characteristics across PPA variants remains unknown. It is also unknown whether [¹⁸F]AV-1451 could have diagnostic utility in differentiating the three PPA variants, and how it would compare to other brain imaging modalities that are currently utilized for diagnostic purposes.

In this study, we aimed to (1) identify the patterns of [¹⁸F]AV-1451 uptake across the three PPA variants, (2) describe region-level patterns of [¹⁸F]AV-1451 uptake in a parsimonious way, independent of clinical diagnosis, and (3) compare [¹⁸F]AV-1451 as a diagnostic tool to other brain imaging modalities that are currently utilized in clinical practice. Our lead hypothesis was that

[¹⁸F]AV-1451 binding characteristics would differ across the three variants and would allow for the separation of lvPPA (3R+4R tauopathy) from the other two variants. To address our specific aims, we performed statistical parametric mapping across the three PPA variants, a principle component analysis based on regional [¹⁸F]AV-1451 uptake to identify patterns independent of clinical diagnosis among 40 prospectively recruited PPA subjects, and penalized multinomial regression to assess for diagnostic utility.

Subjects and Methods

Subjects

Between April 1, 2016 and December 31, 2017, we recruited 42 patients who presented to Mayo Clinic, Department of Neurology with a progressive language disorder who met International Consensus criteria for PPA.³ All 42 patients were recruited as part of an NIH-funded grant that aimed to better understand tau-PET uptake with [¹⁸F]AV-1451 across the PPA variants (PI, Josephs). All patients consented to having their data utilized for research, and the study was approved by the Mayo Clinic Institutional Review Board. Forty-one patients underwent the identical neurological, speech and language, and neuropsychological tests of cognition and completed a 3.0 Tesla (T) volumetric head MRI scan, an [¹⁸F]-fluorodeoxyglucose (FDG)-PET scan, an [¹⁸F]AV-1451 tau-PET scan, and a Pittsburgh compound B (PiB) PET scan to assess for beta-amyloid deposition. One additional patient signed consent but did not complete neuroimaging testing because of claustrophobia and was therefore not included in this study. In addition, 1 PPA patient could not be subclassified into one of the three well-recognized PPA variants.³ As a result, 40 patients were included in this study.

Controls

Using the Mayo Clinic Study of Aging cohort,¹⁷ we identified 80 age- and sex-matched cognitively unimpaired individuals who did not have evidence of amyloid deposition on PiB-PET to serve as a reference group for regional [¹⁸F]AV-1451 levels.¹⁸

Clinical Test Battery

All patients were administered the identical test battery. It included tests of *general cognitive function* (The Montreal Cognitive Assessment),¹⁹ *presence of psychiatric features* (The Neuropsychiatry Inventory-short version),²⁰ *praxis* (Praxis subtest of the Western Aphasia Battery),²¹ *face recognition* (10-item facial recognition task),²² *confrontation naming* (The Sydney Language Test for Naming),²³ *single word comprehension* (The Pyramids and Palm Tree Test–Word-Word version),²⁴ *object knowledge* (The Sydney Language Test for Semantic Association Task),²³ *phonemic fluency* (Letter Fluency Test [FAS]),²⁵ *semantic fluency* (Animal Fluency Test),²⁵ *behavioral control* (The Cambridge Behavioral Inventory),²⁶ *visual perceptual abilities* (The Visual Object and Spatial Battery–Fragmented Letters),²⁷ *visual spatial abilities* (The Visual Object and Spatial Battery–Cube

TABLE 1. Demographic and Clinical Variables Stratified by Diagnosis on the 40 PPA Subjects

Variable ^a	agPPA (N = 13)	lvPPA (N = 14)	svPPA (N = 13)	Total (N = 40)
Male sex (%)	6 (46)	2 (14)	7 (54)	15 (38)
Age at tau scan, y	65 (58, 72)	68 (59, 73)	67 (63, 71)	67 (60, 72)
Global PiB (%)	1.29 (1.20, 1.32)	2.49 (2.19, 2.87)	1.31 (1.25, 1.50)	1.43 (1.27, 2.26)
Right handedness	12 (92)	13 (93)	13 (100)	38 (95)
Disease duration, y	2 (2, 3)	2 (2, 3)	4 (2, 5)	3 (2, 4)
Education	14 (12, 16)	16 (14, 18)	16 (14, 16)	16 (14, 16)
Cambridge Behavioral Inventory/180	34 (18, 48)	16 (13, 26)	46 (34, 64)	33 (14, 58)
Praxis from WAB/60	56 (52, 58)	58 (56, 60)	60 (59, 60)	59 (57, 60)
MDS-UPDRS III/132	4 (2, 9)	2 (2, 4)	0 (0, 3)	2 (0, 5)
Montreal Cognitive Assessment/30	21 (18, 23)	20 (18, 22)	20 (18, 24)	20 (18, 23)
The Neuropsychiatry Inventory/36	5 (3, 10)	2 (0, 3)	7 (4, 11)	4 (2, 8)
Faces recognition/10	10 (10, 10)	10 (9, 10)	4 (1, 7)	10 (7, 10)
Animal fluency	7 (4, 12)	10 (8, 13)	7 (4, 8)	8 (5, 11)
Letter fluency (FAS) sum	8 (5, 10)	29 (24, 32)	25 (17, 30)	25 (17, 32)
SYDBAT naming/30	21 (18, 25)	18 (16, 22)	5 (3, 9)	15 (8, 21)
SYDBAT semantic task/30	24 (20, 28)	27 (24, 27)	14 (10, 19)	22 (15, 27)
Repetition Boston Diagnostic/10	7 (5, 8)	8 (6, 8)	9 (8, 10)	8 (7, 9)
Pyramids & Palm Tree (word-word)/52	46 (42, 49)	49 (48, 51)	39 (38, 42)	45 (40, 49)
Trail making test A, second	55 (47, 90)	51 (44, 70)	48 (29, 58)	50 (39, 69)
Trail making test B, seconds	170 (124, 197)	150 (141, 164)	111 (80, 136)	138 (101, 166)
Rey-O raw score/36	28 (22, 28)	22 (18, 28)	31 (30, 33)	28 (21, 31)
VOSP letters/20	20 (19, 20)	19 (18, 20)	20 (19, 20)	20 (19, 20)
VOSP cubes/10	8 (6, 9)	9 (7, 10)	10 (9, 10)	9 (8, 10)
Digit span	8 (8, 12)	11 (9, 14)	16 (14, 19)	13 (10, 15)
Spatial span	9 (7, 12)	13 (11, 14)	13 (11, 15)	13 (11, 14)
Camden Recognition Memory (faces)/25	22 (18, 24)	24 (22, 24)	20 (18, 23)	22 (18, 24)
Northwestern Anagram Test/10	5 (3, 5)	7 (6, 8)	10 (9, 10)	8 (5, 10)

Summaries are reported as n (percent) or median (25th percentile, 75th percentile).

^aWhere applicable, the maximum score is shown after a slash.

PPA = primary progressive aphasia; PiB = Pittsburgh compound B; VOSP = Visual Object and Space Perceptual Battery; WAB = Western Aphasia Battery; SYDBAT = Sydney Language Battery; MDS-UPDRS III = Movement Disorders Society–Sponsored Revision of the Unified Parkinson's Disease Rating Scale (Motor Examination); agPPA = agrammatic/nonfluent variant; lvPPA = logopenic variant; svPPA = semantic variant.

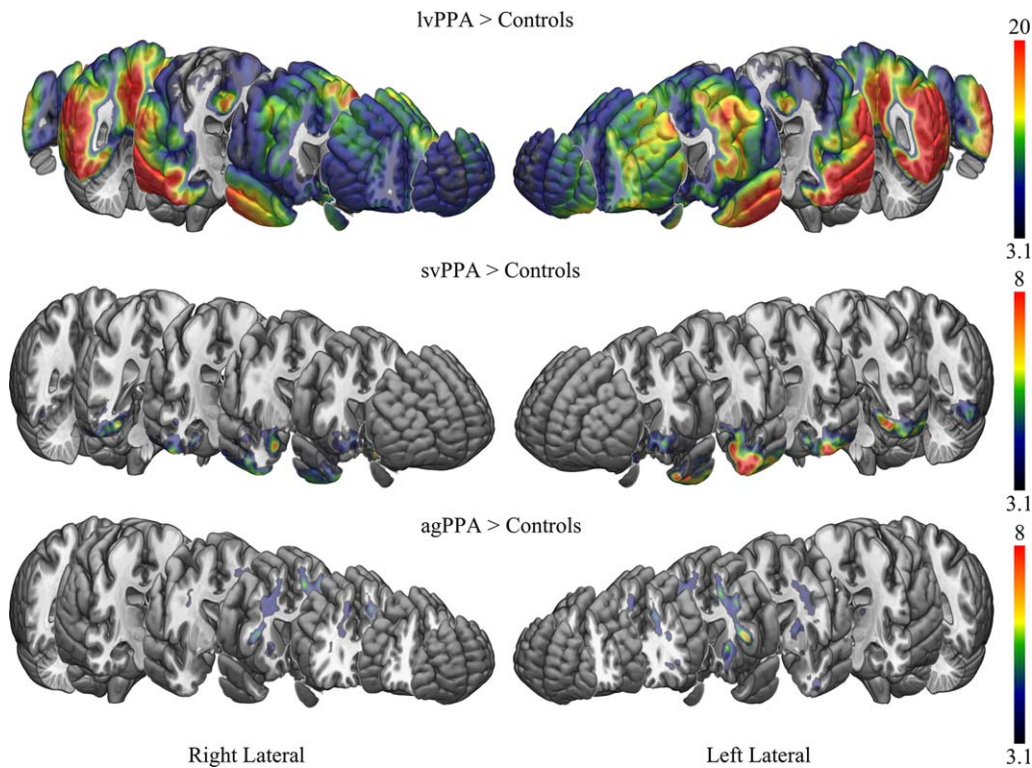


FIGURE 1: [^{18}F]AV-1451 patterns of uptake in the three PPA variants compared to controls. Results are shown after cluster-level correction for multiple comparisons using the family-wise error correction at $p < 0.05$. Results are shown on the MNI152 template using MRICroGL. Scales represent T-score. PPA = primary progressive aphasia; agPPA = agrammatic/nonfluent variant; lvPPA = logopenic variant; svPPA = semantic variant.

analysis)²⁷ and The Rey–Osterrieth complex figure),²⁵ *syntactic ability* (The Northwestern Anagram Test),²⁸ *cognitive speed* (TRAILS Making Test A),²⁵ *executive function* (TRAILS Making Test B),²⁵ *working memory* (Digit Span and Spatial Span),²⁵ *episodic memory* (The Camden Memory Test–Short Recognition Memory Test for faces),²⁹ *sentence repetition* (Repetition subtest of the Boston Diagnostic Aphasia Examination),³⁰ and *motor parkinsonism* (the International Parkinson and Movement Disorder Society–Sponsored Revision of the Unified Parkinson’s Disease Rating Scale–Part III).³¹

PPA Classification

All 40 patients included in this study were evaluated by a behavioral neurologist (K.A.J. or J.G.R.) and had to first meet root diagnostic criteria for PPA^{1,2} to be included in the study. Each patient was then subclassified into one of the three PPA variants based on guidelines from the International Consensus Criteria.³ Diagnoses were made solely on the basis of clinical features and were made independent of the MRI pattern of atrophy, the FDG-PET pattern of hypometabolism, and any results from the [^{18}F]AV-1451 and PiB PET scans. The demographics and clinical features of all 40 PPA patients are shown in Table 1.

Image Acquisition

All PET scans were acquired using a PET/CT (computed tomography) scanner (GE Healthcare, Milwaukee, WI) operating in three-dimensional mode. For tau-PET, an intravenous

bolus injection of approximately 370MBq (range, 333–407) of [^{18}F]AV-1451 was administered, followed by a 20-minute PET acquisition performed 80 minutes after injection. For FDG-PET, subjects were injected with ^{18}F -FDG of approximately 459MBq (range, 367–576), and after a 30-minute uptake period, an 8-minute [^{18}F]-FDG scan was performed. For PiB-PET, subjects were injected with PiB of approximately 628MBq (range, 385–723), and after a 40- to 60-minute uptake period, a 20-minute PiB scan was obtained consisting of four 5-minute dynamic frames following a low-dose CT transmission scan. Standard corrections were applied. Emission data was reconstructed into a 256×256 matrix with a 30-cm field of view (pixel size = 1.0mm; slice thickness = 1.96mm). A global PiB standard uptake value ratio (SUVR) was also generated for each patient in the study, as previously described.³² All subjects had a 3T MPRAGE sequence performed on the same day as the tau-PET, as previously described.³²

Voxel-Level Analysis of [^{18}F]AV-1451 in the PPA Variants

All image processing steps were performed using SPM12 (www.fil.ion.ucl.ac.uk/SPM). Voxel-level analyses of [^{18}F]AV-1451 were performed to address our first aim. The [^{18}F]AV-1451 images were each registered to the subject’s magnetization-prepared rapid gradient echo (MPRAGE) using six degrees-of-freedom registration. Normalization parameters were computed between each MPRAGE and the Mayo Clinic Adult Lifespan

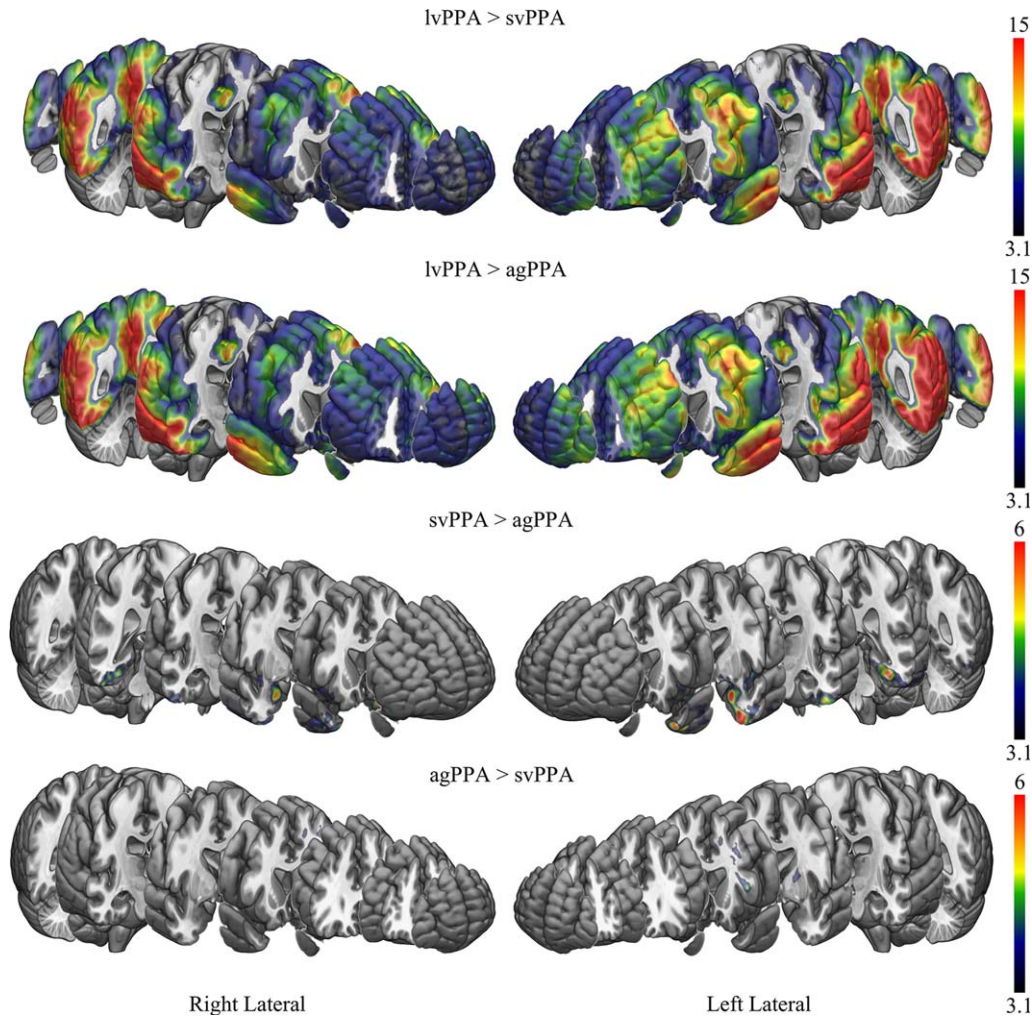


FIGURE 2: [^{18}F]AV-1451 patterns of uptake comparing the PPA variants to each other. Results are shown after cluster-level correction for multiple comparisons using the family-wise error correction at $p < 0.05$. Results are shown on the MNI152 template using MRICroGL. Scales represent T-score. PPA = primary progressive aphasia; agPPA = agrammatic/nonfluent variant; lvPPA = logopenic variant; svPPA = semantic variant.

Template (MCALT) (<https://www.nitrc.org/projects/mcalt/>) using ANTs.³³ With these parameters, the MCALT atlases were propagated to native MPRAGE space, and all voxels in the [^{18}F]AV-1451 image were divided by the median uptake in the cerebellar crus gray matter to create SUVR images. These SUVR images were normalized to the MCALT and smoothed at 6mm full width at half maximum. Voxel-level comparisons were performed comparing each PPA variant to controls using two-sided T-tests in SPM12, with results assessed at $p < 0.05$ after cluster-level correction for multiple comparisons using the family-wise error correction. Age and sex were included in all first aim analyses as covariates.

Generation of Regional Data for Principal Component Analyses

To generate region-level data to be used in our second and third aims, the MCALT atlas was transformed into the native space of each MPRAGE, as in the previous section, and used to calculate regional [^{18}F]AV-1451 uptake and FDG-PET metabolism in both the gray and white matter, as well as gray matter

volumes. For this study, regional values were calculated for the following nine regions-of-interest (ROIs), calculated as voxel weighted medians: *temporal pole* (merged temporal pole mid and temporal pole sup); *lateral temporal cortex* (merged inferior temporal, mid temporal and superior temporal cortices); *entorhinal cortex*; *fusiform cortex*; *orbitofrontal cortex* (merged inferior frontal orbital, mid frontal orbital, superior frontal orbital, and medial frontal orbital); *medial frontal cortex* (merged superior motor area, anterior cingulum, and superior medial frontal); *lateral prefrontal cortex* (merged middle and superior frontal); *Broca's area* (merged inferior frontal operculum and inferior frontal triangularis); and *inferior parietal cortex* (merged inferior parietal, supramarginal, and angular). We selected these ROIs because they are typically involved in the different variants of PPA.^{34,35} The entorhinal cortex was selected to represent the medial temporal lobe, instead of the hippocampus, because hippocampal [^{18}F]AV-1451 measurements can be confounded by off-target uptake in the choroid plexus.^{12,36} Median [^{18}F]AV-1451 and FDG-PET values were calculated from both gray and white matter voxels in each ROI and divided by median uptake

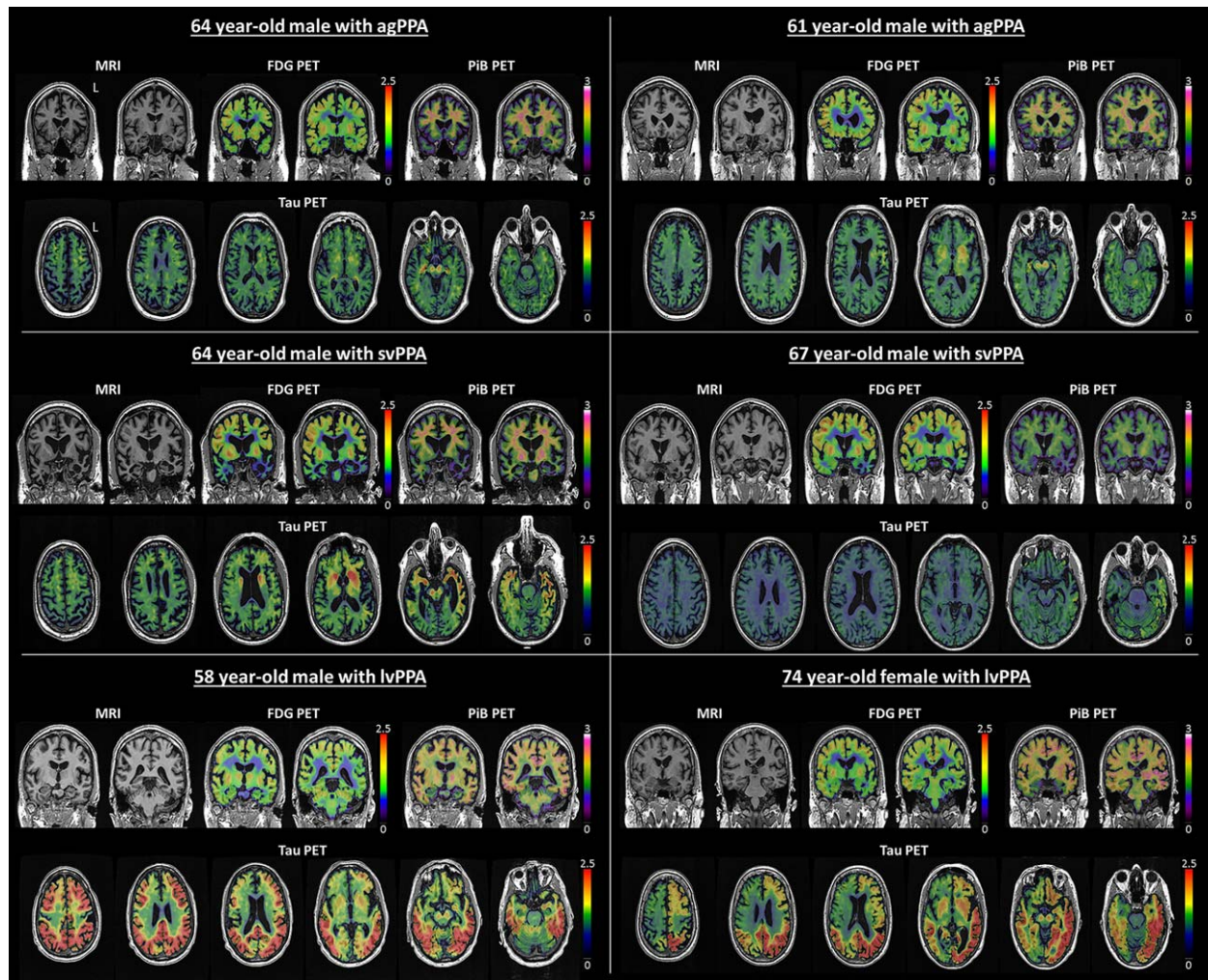


FIGURE 3: Individual [^{18}F]AV-1451 tau-PET, FDG-PET, PiB-PET, and MRI images from 2 agPPA, 2 svPPA, and 2 lvPPA subjects. Scales represent SUVR. FDG = fluorodeoxyglucose; MRI = magnetic resonance imaging; PET = positron emission tomography; PiB = Pittsburgh compound B; PPA = primary progressive aphasia; agPPA = agrammatic/nonfluent variant; lvPPA = logopenic variant; svPPA = semantic variant; SUVR = standard uptake value ratio.

in cerebellar crus ([^{18}F]AV-1451) or pons (FDG-PET) to create SUVRs. We measured signal only in voxels segmented as tissue in order to compensate for differing amounts of atrophy across subjects, without the noise-boosting and atrophy/tau signal mixing effects commonly associated with partial volume correction. Total intracranial volume (TIV) was also calculated by summing SPM12 gray, white, and cerebrospinal fluid segmentations. Log transformed gray matter volumes from each region were then regressed by TIV in 80 healthy age- and sex-matched controls, and standardized residuals were calculated from the model using the log-transformed gray matter volumes for each case. The regional [^{18}F]AV-1451 SUVRs, FDG-PET SUVRs, and standardized gray matter volumes were then each entered into separate principal component analyses as described below.

Principal Component Analyses

To understand and summarize the underlying structure of the ROI-level data, we ran three principal component analyses (PCAs) based on log-transformed [^{18}F]AV-1451 data, log-

transformed FDG-PET data, and standardized magnetic resonance imaging (MRI) gray matter volumes from the 40 PPA patients across nine ROIs listed above in each hemisphere. PCA is an “unsupervised” method in that it is blinded to diagnosis and re-expresses the underlying structure of a data set as a series of distinct, uncorrelated dimensions. The first principal component (PC-1) is a weighted sum of regional data where the weights are chosen so that PC-1 has maximum variation across subjects. PC-1 can be thought of as the “best” single-number summary of the regional data in a given modality. The second principal component (PC-2) is a weighted sum of regional data with weight chosen so that (1) PC-2 is completely uncorrelated with PC-1 and (2) PC-2 has maximum variation after accounting for PC-1. A data set with k variables can be described in terms of k principal components, each accounting for progressively less variation in the data. PCA is a tenable tool in regional analyses because of potential drastic reduction the dimensionality of the data without omitting regions while accounting for collinearity of proximally or functionally related

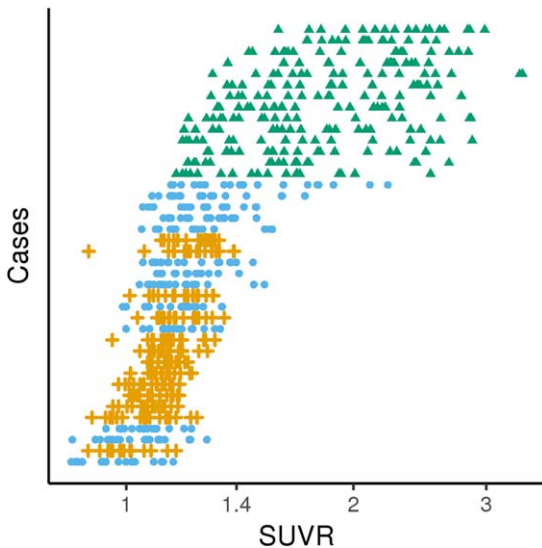


FIGURE 4: [^{18}F]AV-1451 SUVRs for all nine ROIs (left and right), for each hemisphere, on a log scale. The 40 PPA cases are displayed by descending mean SUVR across all 18 ROIs from top to bottom. As can be seen, the lvPPA patients (green triangles) had the highest [^{18}F]AV-1451 SUVRs whereas SUVRs across all ROIs overlapped between agPPA (orange crosses) and svPPA (blue circles) patients. PPA = primary progressive aphasia; agPPA = agrammatic/nonfluent variant; lvPPA = logopenic variant; svPPA = semantic variant; ROIs = regions of interest; SUVR = standard uptake value ratio.

regions. All analyses were done using R³⁷ (version 3.4.1; R Foundation for Statistical Computing, Vienna, Austria).

Voxel-Level Analysis of [^{18}F]AV-1451 Principal Components

In order to provide spatial maps describing the loadings of the principal components in the [^{18}F]AV-1451 analysis, voxel-level correlations were performed in SPM12 between the principal component loadings of each patient and [^{18}F]AV-1451 uptake using the template-space smoothed [^{18}F]AV-1451 images created above. These maps were displayed as unthresholded t statistic maps to show the gradient of positive and negative correlations for loading on each principal component.

Diagnostic Utility of [^{18}F]AV-1451

Penalized multinomial logistic regression was used within each modality to classify cases based on their regional data into the three diagnoses based on their principal component values. Multinomial regression is an extension of binomial logistic regression that allows for more than two outcomes. An optimal ridge penalty determined by leave-one-out cross-validation for each model was used to limit overfitting while retaining all possible predictors (Principal Components) in the model.³⁸ Models were fit within each modality of scan ([^{18}F]AV-1451 PET, FDG-PET, and MRI) with varying numbers of principal components. Cross-modality comparisons were made using the proportion of cases reclassified correctly in models using the same

number of principal components. All analyses were done using R³⁷ (version 3.4.1; R Foundation for Statistical Computing).

Results

Of the 40 PPA patients in this study, 14 met international criteria for lvPPA, 13 for svPPA, and 13 for agPPA. Demographic features were similar across variants, although the majority of the lvPPA patients were female (86%), and svPPA patients' median disease duration was 3 years longer than the other two variants at the time of scan. Each PPA variant showed the expected pattern of impairment on the battery of administered clinical tests. All lvPPA patients showed beta-amyloid deposition on PiB-PET, and this variant had a higher median PiB SUVR compared to the svPPA and agPPA variants (Table 1).

Voxel-Level Analysis of [^{18}F]AV-1451 in the PPA Variants

Voxel-level maps showing [^{18}F]AV-1451 uptake in the three PPA variants compared to controls are shown in Figure 1. The lvPPA group showed significantly higher uptake throughout much of the cortex compared to controls, and compared to svPPA and agPPA (Fig 2). Elevated uptake was particularly observed in the left temporoparietal cortex in lvPPA, with additional involvement of the right temporoparietal cortex and frontal lobes. The svPPA and agPPA groups showed much milder patterns of [^{18}F]AV-1451 uptake compared to controls.

The svPPA group showed elevated [^{18}F]AV-1451 uptake bilaterally in the temporal lobes, involving the temporal pole, inferior and middle temporal gyri, fusiform gyrus, amygdala, parahippocampal gyrus, and entorhinal cortex, with greater uptake observed in the left hemisphere than the right hemisphere, compared to controls. The svPPA group also showed a region of mild elevated uptake that predominantly included bilateral rectus gyrus, orbitofrontal cortex, nucleus accumbens, anterior striatum, and anterior insula compared to controls. The svPPA group showed greater uptake in the temporal pole, amygdala, inferior and middle temporal gyri, fusiform gyrus, parahippocampal gyrus, entorhinal cortex, nucleus accumbens, and anterior insula compared to agPPA (Fig 2). No regions showed greater uptake in svPPA compared to lvPPA.

The agPPA group showed moderately elevated [^{18}F]AV-1451 uptake throughout the white matter of the prefrontal lobe, including orbitofrontal, inferior, middle and superior regions, and temporal lobe, with greater uptake in the left hemisphere, compared to controls. Elevated uptake was also observed in subcortical gray

TABLE 2. Loadings of the First Two Principal Components on Log (tau-PET SUVR) Values

Region	PC1 Loadings	PC2 Loadings
Broca's area L	−0.24	0.21
Broca's area R	−0.22	0.38
Entorhinal cortex L	−0.23	−0.27
Entorhinal cortex R	−0.22	−0.18
Fusiform L	−0.23	−0.32
Fusiform R	−0.23	−0.29
Inferior parietal L	−0.24	−0.10
Inferior parietal R	−0.24	−0.07
Lateral prefrontal L	−0.25	0.20
Lateral prefrontal R	−0.24	0.32
Lateral temporal L	−0.25	−0.21
Lateral temporal R	−0.25	−0.14
Medial frontal L	−0.24	0.19
Medial frontal R	−0.23	0.25
Orbitofrontal L	−0.24	0.18
Orbitofrontal R	−0.22	0.28
Temporal pole L	−0.23	−0.25
Temporal pole R	−0.23	−0.18

PET = positron emission tomography; SUVR = standard uptake value ratio; PC = principal component.

matter structures, including bilateral thalamus, putamen, and globus pallidus, with greater uptake observed in the left hemisphere compared to the right hemisphere. The agPPA group showed greater uptake in the left prefrontal white matter, superior putamen, and thalamus compared to svPPA (Fig 2). No regions showed greater uptake in agPPA compared to lvPPA.

Representative [^{18}F]AV-1451 images for each of the three PPA variants are shown in Figure 3.

Principal Component Analysis of [^{18}F]AV-1451, FDG-PET, and MRI

Figure 4 shows the actual [^{18}F]AV-1451 SUVRs for all PPA patients. All 14 lvPPA patients had higher mean SUVRs than any of the agPPA and svPPA patients, who tended to be intermixed. The [^{18}F]AV-1451 PCA suggested an underlying two-dimensional structure in the regional data given that the first component accounted for 81% (standard deviation [SD], 3.83) of the variation and the second component accounted for an additional

7% (SD, 1.15). Table 2 shows the loadings of these two principal components for the ROIs, and Figure 5 shows voxel-level correlations between [^{18}F]AV-1451 uptake and the loadings of the two principal components. We interpret the first principal component (PC-1) as an overall tau severity measure given that the ROI loadings are all of the same sign and essentially the same magnitude. The voxel-level maps similarly illustrate a negative correlation between the loading on PC-1 and [^{18}F]AV-1451 in much of the cortex, particularly in temporoparietal and frontal regions (Fig 5), implying that a greater negative loading is associated with greater [^{18}F]AV-1451 binding in these areas. We interpret the second principal component (PC-2) as a dimension representing a contrast between frontal and temporal regions. That is, after accounting for severity summarized in PC-1, PC-2 locates individuals on a spectrum ranging from relatively high temporal uptake and relatively low frontal uptake to relatively low temporal uptake and relatively high frontal uptake. This is illustrated in Figure 5 where a negative correlation is observed between PC-2 loading and medial and lateral temporal lobe [^{18}F]AV-1451 uptake, and a positive correlation between loadings and uptake in the prefrontal cortex.

The plot in Figure 6 shows the separation of the three PPA variants according to PC-1 and PC-2 that were calculated from the PCA using the ROI data from each of the three modalities. For [^{18}F]AV-1451, all lvPPA patients were more severe than average (ie, to the left of the mean on the PC-1 axis in Fig 6) with this dimension discriminating perfectly between lvPPA and the other two variants (area under the receiver operator curve = 1; $p < 0.001$). After accounting for severity, if we look at the PC-2 axis, we see perfect separation of the agPPA and svPPA patients (area under the receiver operator curve = 1; $p < 0.001$). In other words, a combination of higher uptake in frontal regions and relatively reduced uptake in temporal regions effectively distinguish agPPA and svPPA.

The penalized multinomial logistic regression models show that [^{18}F]AV-1451 outperformed both FDG-PET and MRI when using two principal components (Fig 6). When considering from three to seven principal components, [^{18}F]AV-1451 and FDG-PET were comparable while both consistently outperformed MRI (Fig 6). These penalized models provide a fair estimate of the ability of these different scan modalities to discriminate between these three diagnoses, showing stronger signals in [^{18}F]AV-1451 and FDG-PET than MRI.

Discussion

[^{18}F]AV-1451 patterns of uptake were different across the three PPA variants, as we had hypothesized. The

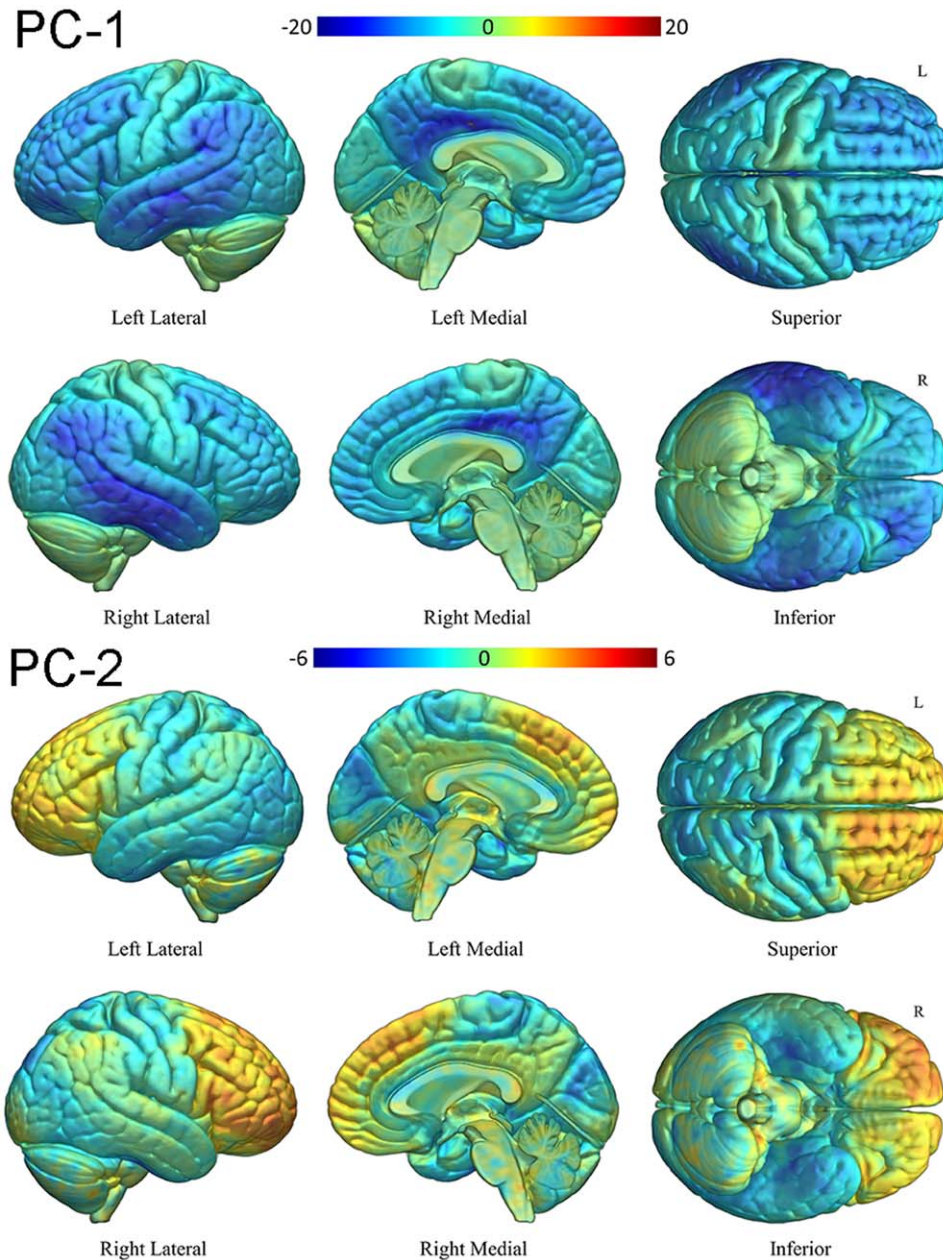


FIGURE 5: T-maps for the correlation between PC-1 and PC-2 loading and voxel-wise [^{18}F]AV-1451 uptake, with cool colors showing regions of negative correlation (ie, voxels where a lower PC load is associated with higher [^{18}F]AV-1451 uptake) and warm colors showing regions of positive correlation. PC = principal component.

patterns differed in terms of severity of binding, regions of uptake, and relative involvement of gray versus white matter. Taking all these differences into account, we show that [^{18}F]AV-1451 patterns of uptake can be utilized to predict clinical diagnosis of the PPA variants at a single subject level with a relatively high degree of accuracy. We found [^{18}F]AV-1451 PET to be as good as FDG-PET and better than MRI at predicting clinical diagnosis.

One of the most striking observations of the study was the significant amount of [^{18}F]AV-1451 uptake in the lvPPA variant compared to controls and compared to svPPA and agPPA. Three other small case series have also

observed uptake of [^{18}F]AV-1451 in lvPPA.^{39–41} Given that autoradiographic studies show [^{18}F]AV-1451 binds strongly to 3R+4R tau, and the fact that pathological studies have found lvPPA is associated with 3R+4R tau, it is reasonable to deduce that [^{18}F]AV-1451 uptake in lvPPA would highly correlate with tau burden in the brain at the time of scan. Further supporting this notion is the fact that the asymmetric uptake, most severely involving the left temporoparietal cortex, that we observed with [^{18}F]AV-1451 uptake in lvPPA is similar to what has been observed in pathological studies of tau neurofibrillary tangle deposition in lvPPA.^{8,42} The

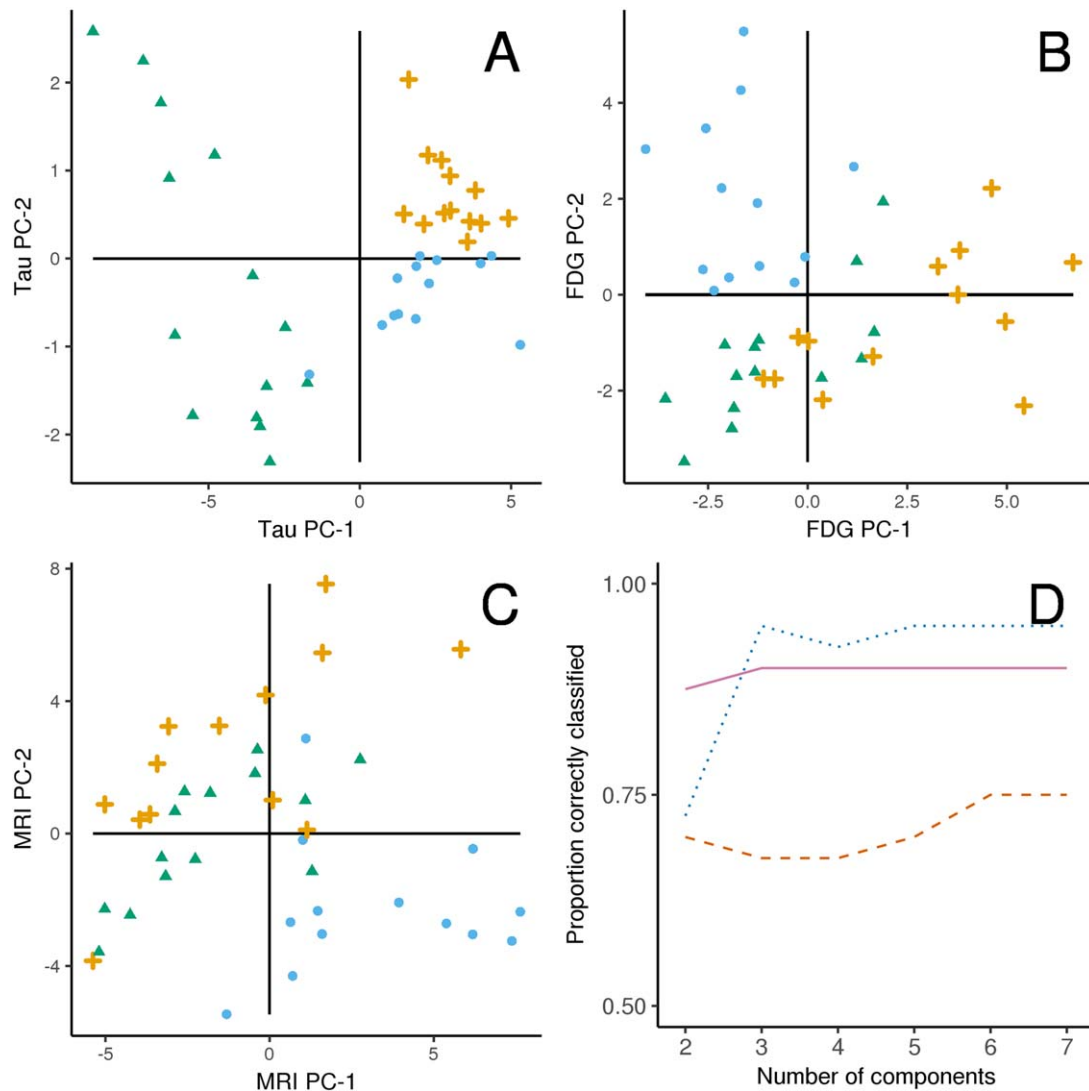


FIGURE 6: Plots illustrating the results of the principal component (PC) analyses for [^{18}F]AV-1451 uptake (A), FDG-PET metabolism (B), and MRI volumes (C). Each plot shows the three PPA variants according to the first two principal components within a modality, with PC-1 on the x-axis and PC-2 on the y-axis. The three PPA variants, lvPPA (green triangles), agPPA (orange crosses), and svPPA (blue circles), separate perfectly with [^{18}F]AV-1451 with two principal components, with less than perfect separation in FDG-PET and MRI modalities. (D) compares penalized multinomial regression models containing increasing numbers of components on the x-axis by their predictive accuracy on the y-axis in these 40 cases. With two components, tau-PET (solid violet line) classification is the highest whereas with three or more components FDG-PET (dotted blue line) shows the best discrimination. MRI (dashed red line) had the lowest classification accuracy in all instances. FDG = fluorodeoxyglucose; MRI = magnetic resonance imaging; PET = positron emission tomography; PPA = primary progressive aphasia; agPPA = agrammatic/nonfluent variant; lvPPA = logopenic variant; svPPA = semantic variant.

regions of increased uptake identified in our lvPPA patients were similar to the regions reported in the three other [^{18}F]AV-1451 studies and are the same regions that are structurally and functionally most involved in lvPPA.^{39–41} The degree of [^{18}F]AV-1451 uptake observed in lvPPA is not likely to reflect clinical severity given that performance on a test of general cognitive performance, as well as disease duration, was similar in lvPPA compared to the other two groups.

Unlike with lvPPA, [^{18}F]AV-1451 uptake in svPPA was more focal, predominantly involving regions of the

temporal lobe, as well as ventromedial frontal regions, that are often atrophic and functionally impaired in svPPA.⁴³ Given that pathological studies have identified TDP-43, and not tau, as being most strongly associated with svPPA,^{6,8,10} and autoradiographic studies of svPPA with TDP-43 have found little evidence for [^{18}F]AV-1451 binding,^{12–14} it is unclear what elevated [^{18}F]AV-1451 uptake represents in svPPA. The regions that showed uptake in our studies were also reported to be involved in two other studies of [^{18}F]AV-1451 uptake in svPPA,^{44,45} and one study with a different ligand,

THK-5351.⁴⁶ Therefore, it is worthwhile to consider carefully what [¹⁸F]AV-1451 may be binding to in svPPA. Further arguing against [¹⁸F]AV-1451 simply binding to TDP-43 is the fact that TDP-43 deposition in svPPA also occurs to a similar density in regions outside of those that showed [¹⁸F]AV-1451 uptake, such as the middle frontal and inferior parietal cortex.¹⁰ We cannot exclude the possibility that there is some focal 3R+4R, 3R or 4R tau that is being detected by [¹⁸F]AV-1451 in svPPA. We also have to consider the possibility of some off-target binding to something that is focally present in the regions of most severe neurodegeneration such as heme by-products, iron, calcium, or something else. Regardless, off-target binding is a very plausible explanation for some of the uptake in svPPA given that elevated uptake of [¹⁸F]AV-1451 has been observed in meningiomas, vascular malformations, and infarctions, for example,^{47,48} where there is no good evidence that 3R+4R tau is present.

Similar to svPPA, [¹⁸F]AV-1451 uptake in agPPA was less robust and more focal compared to lvPPA. Uptake was observed in frontal and basal ganglia regions that are typically atrophic and functionally impaired in agPPA. What was most noticeable regarding [¹⁸F]AV-1451 uptake in agPPA was that uptake in the frontal lobes was limited to white matter. This suggests that whatever [¹⁸F]AV-1451 is binding to in agPPA maybe more strongly associated with the subcortical white matter, than the cortical gray matter. We also observed greater [¹⁸F]AV-1451 uptake in subcortical gray matter structures in agPPA compared to controls and svPPA. More specifically, we noted elevated uptake in the thalamus, globus pallidus, and putamen. Off-target binding of the ligand has been observed in these subcortical structures in healthy controls¹² and typically increases with age.⁴⁹ However, because we compared our patients to age-matched healthy, PiB-negative controls, it is possible that this finding is disease specific. Involvement of the thalamus, globus pallidus, and putamen is reminiscent of the pattern of [¹⁸F]AV-1451 uptake that has been observed in another neurodegenerative syndrome, Richardson's syndrome.^{49,50} Intriguingly, both agPPA and Richardson's syndrome are strongly associated with 4R tauopathies. It is unclear, however, whether [¹⁸F]AV-1451 binds to 4R tau.^{12–15} We suspect that whatever target [¹⁸F]AV-1451 is binding to in agPPA may be similar, or identical to the target in Richardson's syndrome. It is less clear whether the binding targets are similar between agPPA and svPPA (a non-4R tauopathy).

The elevated uptake of [¹⁸F]AV-1451 in the three PPA variants is worthy of further discussion. Uptake in

svPPA and agPPA challenges the notion that [¹⁸F]AV-1451 binding is 100% specific to tau, and argues that the ligand has incomplete specificity. Therefore, although binding in lvPPA is likely to highly correlate with underlying 3R+4R tau, there is a high chance that even in lvPPA uptake reflects the sum of specific and nonspecific binding; a similar situation may be occurring in agPPA and svPPA. With that said, the findings from this study are still valuable and significant because [¹⁸F]AV-1451 uptake did provide excellent discrimination of the three PPA variants.

Our analyses to examine the underlying structure of the regional data showed that [¹⁸F]AV-1451 uptake was clearly distinct in terms of severity with lvPPA showing elevated uptake compared to svPPA and agPPA. This suggests that given a diagnosis of PPA, predicting lvPPA based on [¹⁸F]AV-1451 requires only taking into account the degree of uptake across these nine ROIs. It was unnecessary to consider the specific pattern of uptake in order to predict lvPPA, although we could hypothesize that accounting for pattern could provide even greater predictive value for lvPPA cases, especially those cases that show relatively lower degrees of [¹⁸F]AV-1451 uptake. The degree of tau uptake did not, however, allow prediction of svPPA over agPPA; this is where the contrasting pattern of frontal versus temporal [¹⁸F]AV-1451 uptake was useful. Based on results from this study, it appears that a pattern of [¹⁸F]AV-1451 uptake that involves frontal regions more than temporal regions suggests a diagnosis of agPPA over svPPA, whereas a pattern of [¹⁸F]AV-1451 uptake that involves the anteromedial temporal lobe regions more than the frontal regions suggests a diagnosis of svPPA. Therefore, although [¹⁸F]AV-1451 may prove not to be a stand-alone diagnostic tool to predict the underlying pathologies of the PPA variants, the degree and patterns of uptake may still be helpful to differentiate the variants.

We compared the diagnostic utility of [¹⁸F]AV-1451 to FDG-PET and MRI volumes, given that both modalities are commonly utilized in clinical practice to distinguish between PPA variants. [¹⁸F]AV-1451 was found to be as good as FDG-PET, and better than MRI, to discriminate between PPA variants. In fact, one could argue that [¹⁸F]AV-1451 is the best of the three imaging modalities, given that with just two principal components it had the best discriminatory value, and the fact that the loadings showed that a simple diagnostic algorithm first accounting for uptake severity followed by frontal versus temporal uptake was all that was needed for almost perfect prediction; similar predictive power with FDG-PET required at least three principal components. Regardless, these findings further support the notion that [¹⁸F]AV-1451 may be a useful added

diagnostic tool in PPA and could provide added diagnostic value with multimodality imaging, that is, [^{18}F]AV-1451, FDG-PET, and MRI.

The strengths of this study are that all patients were well characterized clinically and that all 120 patients and healthy controls underwent identical imaging protocols. Holding acquisition and analysis parameters constant allows for a more confident comparison of results. In addition, our PCA was unsupervised, allowing us to assess variability in uptake, metabolism, and volumes unbiased by clinical diagnosis. The lack of autopsy confirmation is a limitation and it is possible that some of our agPPA and svPPA patients may share the same underlying pathology, such as Pick's disease, in which [^{18}F]AV-1451 binding characteristics are unknown and autoradiographic findings are unclear.¹² Other limitations of this study include the relatively small sample size and the possibility of participation or other selection biases.

The findings from this study reveal that [^{18}F]AV-1451 has potential to differentiate the PPA variants and to be utilized as a diagnostic tool. However, the lack of a credible biological explanation for the elevated uptake in svPPA and agPPA make it less appealing as a biomarker, at present. What is critically needed is to understand what the ligand is binding to in cases that lack pathological evidence for the presence of 3R+4R tau.

Acknowledgment

This study was funded by NIH grants R21-NS94684, R01-AG50603, R01-DC12519, and U01 AG006786, Mayo Clinic Radiology Research, and support from the Elsie and Marvin Dekelboum Family Foundation.

We acknowledge AVID Radiopharmaceuticals for provision of AV-1451 precursor, chemistry production advice and oversight, and FDA regulatory cross-filing permission and documentation needed for this work.

Author Contributions

K.A.J., P.R.M., S.D.W., and J.L.W. contributed to the conception and design of the study. K.A.J., P.R.M., H.B., C.G.S., J.R.D., H.M.C., M.M.M., J.G.R., S.D.W., M.L.S., R.L.U., D.A.D., B.F.B., D.T.J., D.S.K., R.C.P., C.R.J., V.J.L., and J.L.W. contributed to the acquisition and analysis of data. K.A.J. contributed to drafting the manuscript.

Potential Conflicts of Interest

Nothing to report.

References

1. Mesulam MM. Slowly progressive aphasia without generalized dementia. *Ann Neurol* 1982;11:592–598.
2. Mesulam MM. Primary progressive aphasia. *Ann Neurol* 2001;49:425–432.
3. Gorno-Tempini ML, Hillis AE, Weintraub S, et al. Classification of primary progressive aphasia and its variants. *Neurology* 2011;76:1006–1014.
4. Josephs KA, Duffy JR, Strand EA, et al. Clinicopathological and imaging correlates of progressive aphasia and apraxia of speech. *Brain* 2006;129(pt 6):1385–1398.
5. Deramecourt V, Lebert F, Debachy B, et al. Prediction of pathology in primary progressive language and speech disorders. *Neurology* 2010;74:42–49.
6. Josephs KA, Hodges JR, Snowden JS, et al. Neuropathological background of phenotypical variability in frontotemporal dementia. *Acta Neuropathol* 2011;122:137–153.
7. Spinelli EG, Mandelli ML, Miller ZA, et al. Typical and atypical pathology in primary progressive aphasia variants. *Ann Neurol* 2017;81:430–443.
8. Mesulam MM, Weintraub S, Rogalski EJ, et al. Asymmetry and heterogeneity of Alzheimer's and frontotemporal pathology in primary progressive aphasia. *Brain* 2014;137(pt 4):1176–1192.
9. Goedert M, Spillantini MG, Jakes R, Rutherford D, Crowther RA. Multiple isoforms of human microtubule-associated protein tau: sequences and localization in neurofibrillary tangles of Alzheimer's disease. *Neuron* 1989;3:519–526.
10. Josephs KA, Stroh A, Dugger B, Dickson DW. Evaluation of subcortical pathology and clinical correlations in FTL-DU subtypes. *Acta Neuropathol* 2009;118:349–358.
11. Xia CF, Arteaga J, Chen G, et al. [(18)F]T807, a novel tau positron emission tomography imaging agent for Alzheimer's disease. *Alzheimers Dement* 2013;9:666–676.
12. Lowe VJ, Curran G, Fang P, et al. An autoradiographic evaluation of AV-1451 Tau PET in dementia. *Acta Neuropathol Commun* 2016;4:58.
13. Marquie M, Normandin MD, Vanderburg CR, et al. Validating novel tau positron emission tomography tracer [F-18]-AV-1451 (T807) on postmortem brain tissue. *Ann Neurol* 2015;78:787–800.
14. Sander K, Lashley T, Gami P, et al. Characterization of tau positron emission tomography tracer [18F]AV-1451 binding to postmortem tissue in Alzheimer's disease, primary tauopathies, and other dementias. *Alzheimers Dement* 2016;12:1116–1124.
15. Marquie M, Normandin MD, Meltzer AC, et al. Pathological correlations of [F-18]-AV-1451 imaging in non-Alzheimer tauopathies. *Ann Neurol* 2017;81:117–128.
16. Josephs KA, Whitwell JL, Tacik P, et al. [18F]AV-1451 tau-PET uptake does correlate with quantitatively measured 4R-tau burden in autopsy-confirmed corticobasal degeneration. *Acta Neuropathol* 2016;132:931–933.
17. Roberts RO, Geda YE, Knopman DS, et al. The Mayo Clinic Study of Aging: design and sampling, participation, baseline measures and sample characteristics. *Neuroepidemiology* 2008;30:58–69.
18. Lowe V, Wiste H, Senjem M, et al. Widespread brain tau on molecular imaging and its association with aging, Braak stage, and Alzheimer's dementia. *Brain* 2018;141:271–287.
19. Nasreddine ZS, Phillips NA, Bedirian V, et al. The Montreal Cognitive Assessment, MoCA: a brief screening tool for mild cognitive impairment. *J Am Geriatr Soc* 2005;53:695–699.
20. Kaufer DI, Cummings JL, Ketchel P, et al. Validation of the NPI-Q, a brief clinical form of the Neuropsychiatric Inventory. *J Neuropsychiatry Clin Neurosci* 2000;12:233–239.

21. Kertesz A. Western Aphasia Battery (Revised). San Antonio, TX: PsychCorp; 2007.
22. Josephs KA, Duffy JR, Strand EA, et al. Characterizing a neurodegenerative syndrome: primary progressive apraxia of speech. *Brain* 2012;135(pt 5):1522–1536.
23. Savage S, Hsieh S, Leslie F, et al. Distinguishing subtypes in primary progressive aphasia: application of the Sydney language battery. *Dement Geriatr Cogn Disord* 2013;35:208–218.
24. Howard D, Patterson K. *Pyramids and Palm Trees: a test of semantic access from pictures and words*. Bury St Edmunds, UK: Thames Valley; 1992.
25. Lezak MD, Howieson DB, Bigler ED, Tranel D. *Neuropsychological Assessment*, 5th ed. New York, NY: Oxford University Press; 2012.
26. Bozeat S, Gregory CA, Ralph MA, Hodges JR. Which neuropsychiatric and behavioural features distinguish frontal and temporal variants of frontotemporal dementia from Alzheimer's disease? *J Neurol Neurosurg Psychiatry* 2000;69:178–186.
27. Warrington EK, James M. *The visual object and space perception battery*. Bury St Edmunds, UK: Thames Valley; 1991.
28. Weintraub S, Mesulam MM, Wieneke C, et al. The Northwestern Anagram Test: measuring sentence production in primary progressive aphasia. *Am J Alzheimers Dis Other Dement* 2009;24:408–416.
29. Clegg F, Warrington EK. Four easy memory tests for older adults. *Memory* 1994;2:167–182.
30. Goodglass H, Kaplan E, Barresi B. *The Boston Diagnostic Aphasia Examination (BDAX)*. Baltimore, MD: Lippincott, Williams and Wilkins; 2001.
31. Goetz CG, Tilley BC, Shaftman SR, et al. Movement Disorder Society-sponsored revision of the Unified Parkinson's Disease Rating Scale (MDS-UPDRS): scale presentation and clinimetric testing results. *Mov Disord* 2008;23:2129–2170.
32. Jack CR Jr, Lowe VJ, Senjem ML, et al. 11C PiB and structural MRI provide complementary information in imaging of Alzheimer's disease and amnesic mild cognitive impairment. *Brain* 2008;131(pt 3):665–680.
33. Avants BB, Epstein CL, Grossman M, Gee JC. Symmetric diffeomorphic image registration with cross-correlation: evaluating automated labeling of elderly and neurodegenerative brain. *Med Image Anal* 2008;12:26–41.
34. Botha H, Duffy JR, Whitwell JL, et al. Classification and clinicoradiologic features of primary progressive aphasia (PPA) and apraxia of speech. *Cortex* 2015;69:220–236.
35. Rabinovici GD, Jagust WJ, Furst AJ, et al. Abeta amyloid and glucose metabolism in three variants of primary progressive aphasia. *Ann Neurol* 2008;64:388–401.
36. Ikonomic MD, Abrahamson EE, Price JC, Mathis CA, Klunk WE. [¹⁸F]AV-1451 positron emission tomography retention in choroid plexus: more than "off-target" binding. *Ann Neurol* 2016;80:307–308.
37. R Core team. *R: A language and environment for statistical computing*. Vienna: R Foundation for Statistical Computing; 2017.
38. Hastie T, Tibshirani R, Friedman JH. *The Elements of Statistical Learning: Data Mining, Inference, and Prediction: with 200 Full-Color Illustrations*. New York, NY: Springer; 2001.
39. Nasrallah IM, Chen YJ, Hsieh MK, et al. 18F-Flortaucipir PET-MRI correlations in non-amnesic and amnesic variants of Alzheimer disease. *J Nucl Med* 2018;59:299–306.
40. Ossenkoppele R, Schonhaut DR, Scholl M, et al. Tau PET patterns mirror clinical and neuroanatomical variability in Alzheimer's disease. *Brain* 2016;139(pt 5):1551–1567.
41. Xia C, Makaretz SJ, Caso C, et al. Association of In Vivo [¹⁸F]AV-1451 tau PET imaging results with cortical atrophy and symptoms in typical and atypical Alzheimer disease. *JAMA Neurol* 2017;74:427–436.
42. Josephs KA, Dickson DW, Murray ME, et al. Quantitative neurofibrillary tangle density and brain volumetric MRI analyses in Alzheimer's disease presenting as logopenic progressive aphasia. *Brain Lang* 2013;127:127–134.
43. Mumme CJ, Patterson K, Price CJ, et al. A voxel-based morphometry study of semantic dementia: relationship between temporal lobe atrophy and semantic memory. *Ann Neurol* 2000;47:36–45.
44. Bevan-Jones WR, Cope TE, Jones PS, et al. [¹⁸F]AV-1451 binding in vivo mirrors the expected distribution of TDP-43 pathology in the semantic variant of primary progressive aphasia. *J Neurol Neurosurg Psychiatry* 2017 Sep 14. pii: jnnp-2017-316402. doi: 10.1136/jnnp-2017-316402. [Epub ahead of print]
45. Makaretz SJ, Quimby M, Collins J, et al. Flortaucipir tau PET imaging in semantic variant primary progressive aphasia. *J Neurol Neurosurg Psychiatry* 2017 Oct 06. pii: jnnp-2017-316409. doi: 10.1136/jnnp-2017-316409. [Epub ahead of print]
46. Lee H, Seo S, Lee SY, et al. [¹⁸F]-THK5351 PET imaging in patients with semantic variant primary progressive aphasia. *Alzheimer Dis Assoc Disord* 2017 Oct 12. doi: 10.1097/WAD.0000000000000216. [Epub ahead of print]
47. Lockhart SN, Ayakta N, Winer JR, et al. Elevated 18F-AV-1451 PET tracer uptake detected in incidental imaging findings. *Neurology* 2017;88:1095–1097.
48. Bruinsma TJ, Johnson DR, Fang P, et al. Uptake of AV-1451 in meningiomas. *Ann Nucl Med* 2017;31:736–743.
49. Cho H, Choi JY, Hwang MS, et al. Subcortical 18 F-AV-1451 binding patterns in progressive supranuclear palsy. *Mov Disord* 2017;32:134–140.
50. Whitwell JL, Lowe VJ, Tosakulwong N, et al. [¹⁸F]AV-1451 tau positron emission tomography in progressive supranuclear palsy. *Mov Disord* 2017;32:124–133.